Characterizing Quantum-Dot Cellular Automata

Burkhard Ritter
Supervised by Prof. Dr. Kevin Beach

May 2014

Contents

1 Approximations **5**

1.1 Fixed charge model 5

1.2 Bond model 6

1.3 Ising model 7

1.4 Validity of the approximations 13

Chapter 1

Approximations

1.1 Fixed charge model

Exact diagonalization scales exponentially with system size. For the full *grand canonical* QCA Hamiltonian, Eq. **??**, only QCA devices of up to two cells are computationally feasible. Therefore, to access larger systems we need to introduce approximations. Approximating means to simplify. However, by carefully establishing successive approximations and their limits, we also reduce the problem to its essential ingredients and thus, hopefully, we gain a better understanding of the system. As a first step, we reduce the Hilbert space to a *fixed* number of particles per cell. We disallow any charge fluctuations, both for the system as a whole and for each individual cell. With that, we omit the chemical potential term in the Hamiltonian, $\mu = 0$, and prohibit inter-cell hopping. This is a major simplification. However, it is in line with the QCA idea: The approach requires a fixed number of charges per cell, typically two electrons, and cells are thought to interact only via Coulomb forces. In a sense we are shifting the starting point of our investigation. If the *fixed* charge approximation is not valid for a given system, then there is no hope of implementing QCA on it. On the other hand, for experimental systems like the atomic silicon quantum dots and for a given cell layout, it should always be possible, at least in principle, to tune the system parameters, especially the chemical potential, to get the system into the right particle number sector. The system has to be set up in a way that the two-electrons-per-cell sector is lowest in energy and other particle number sectors are sufficiently gapped out, that is, at an energy, compared to the ground state energy, much larger than temperature. Of course, in practice there are very clear limits as to how much the system parameters can be tuned and any QCA cell layout considered within the *fixed* charge approximation cannot necessarily be readily implemented on a given real-world material system.

For the *fixed* charge system, the state space scales as $N_s = \binom{8}{2}^{N_c} = 28^{N_c}$ (N_c is the number of cells). Using symmetries, the largest block of the Hamiltonian matrix is the spin zero sector, of size $N_s' = 16^{N_c}$. On conventional computer hardware, systems of

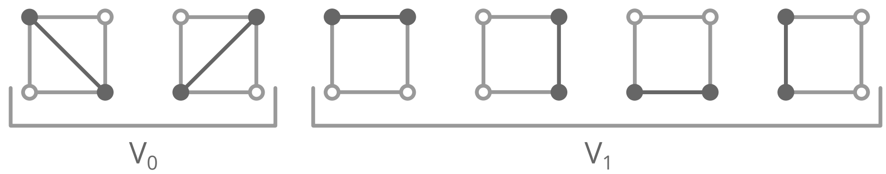

Figure 1.1: ...

up to four cells are possible, with memory requirements of 32GB. In practice, however, calculations for four-cell systems take too long and thus three cells is the practical limit for the *fixed*-number-of-particles-per-cell model.

1.2 Bond model

At its heart, QCA is a semi-classical idea. It relies solely on charge-charge interactions and ignores the particle spins. Therefore, as a next step in our quest to access larger system sizes, we neglect the spin degree of freedom in our model. The 28 states per cell of the *fixed* charge model can be reorganized into four doubly occupied dots and six bonds. The six bonds are illustrated in Fig. 1.1. Each bond corresponds to one spin singlet and three spin triplet states. The *bond* approximation only keeps one state for each bond and discards the doubly occupied states as well. With the *bond* model we thus assume that singlet and triplet states are qualitatively equivalent and energetically degenerate, and that doubly occupied dots are sufficiently gapped out, that is, $U \gg T$. As QCA ignores the spin, singlets and triplets should be qualitatively equivalent, but they are not quite degenerate. We expect that virtual double-occupancy lowers the energies of the singlet states and therefore introduces a small singlet-triplet splitting. Still, degeneracy is presumably not a bad assumption to start with and we will look at the singlet-triplet splitting in detail in due course. For the *bond* model the QCA Hamiltonian reduces to

$$H = -\sum_{\langle ij \rangle} t c_i^\dagger c_j + \sum_{i<j} V_{ij} \left(n_i - q\right)\left(n_j - q\right) . \tag{1.1}$$

With six bond states per cell, the Hilbert space of the *bond* model is $N_s = 6^{N_c}$ (N_c the number of cells). Five and six cells are doable, with memory requirements of 460MB and 16GB, respectively, but for practical calculations five cells really is the limit. For the *bond* model there are no symmetries that can be exploited.

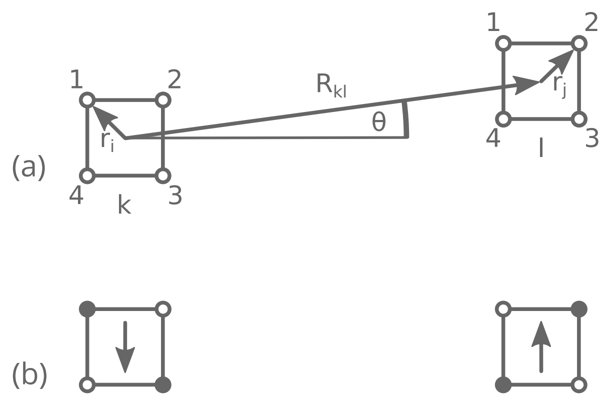

Figure 1.2: a) QCA cells k and l. b) The two-states-per-cell approximation identifies each cell with a spin ↑ or ↓.

1.3 Ising model

A linear array of QCA cells where each cell has a state of logic 0 or 1 is reminiscent of a 1D spin $\frac{1}{2}$ chain. Indeed, if we reduce the basis to only two states per cell, down from six states in the *bond* picture, we can map the QCA system to a transverse-field Ising model with long-ranging interactions. This is an attractive proposition: The smaller Hilbert space allows for larger system sizes with our exact diagonalization method; more importantly, the transverse-field Ising model is amenable to sign-problem-free Stochastic series expansion (SSE) quantum Monte Carlo schemes [1]. These methods do not scale exponentially[1] and consequently allow access to much larger systems. Last, but not least, such a mapping connects the QCA approach to the established and well studied Ising model. The prospect hinges on the assumption that the two-states-per-cell basis actually is a good approximation for QCA systems. And while bistable two-state cells are certainly the picture we have in mind when we talk about QCA, it is not *a priori* clear whether this is a correct physical picture.

We use the *bond* Hamiltonian (1.1) as the starting point. We had already discussed in the last chapter that such a Hamiltonian can be decomposed into single-cell terms and cell-cell interaction terms,

$$H = \sum_k H_k^c + \sum_{k<l} H_{kl}^{cc} \,. \tag{1.2}$$

In comparison, the transverse field Ising model is described by

$$\tilde{H} = -\sum_k \gamma S_k^x + \sum_{k<l} J_{kl} S_k^z S_l^z \,. \tag{1.3}$$

[1]SSE quantum Monte Carlo methods roughly scale as $N \ln N$ where N is the system size.

Thus, we would like to map the single cell term H_k^c to the transverse field term $-\gamma S_k^x$ and the Coulombic cell-cell interaction H_{kl}^{cc} to the Ising term $J_{kl} S_k^z S_l^z$. Each cell k is identified with a pseudo spin S_k^z, specifically the logic 0 with a spin down state and the logic 1 with a spin up state, as illustrated in Fig. 1.2(b). We will first look at how the QCA cell can be represented by only two states and derive an approximate expression for the transverse field γ. Then we will use a multipole expansion to derive J_{kl} from the cell-cell Coulomb interaction.

To arrive at a single-cell-basis with only two states we can, in principle, follow a similar prescription as for the fixed charge and bond approximations: We neglect high energy states which are assumed to be gapped out. In this case these are the four edge states with Coulomb energy V_1, $|\psi_Q\rangle = \{|3\rangle, |4\rangle, |5\rangle, |6\rangle\}$ in Fig. 1.1, where we have introduced $|\psi_Q\rangle$ to denote the high-energy subspace of the single-cell Hilbert space. We only keep the low-energy, diagonal states $|\psi_P\rangle = \{|1\rangle, |2\rangle\}$ with Coulomb energy V_0. Of course, these two are exactly our logic 0 and logic 1 state, or $|1\rangle \doteq |\downarrow\rangle$ and $|2\rangle \doteq |uparrow\rangle$, respectively. Here, $|\psi_P\rangle$ denotes the low-energy subspace. For the high-energy states to be sufficiently gapped out we require $\Delta V = V_1 - V_0 \gg T$. In contrast to the fixed charge and bond models, merely truncating the Hilbert space is not sufficient for the Ising model. For our previous two approximations the Hamiltonian had remained essentially unchanged, apart from dropping no longer relevant terms, such as the chemical potential term or the Hubbard U term. The retained states were exactly the same states as in the full, untruncated model. But with only two states per cell the existing Hamiltonian (1.1) does not "work": There is no process that takes the system from state $|1\rangle$ to $|2\rangle$. Therefore, for the Ising approximation we need to derive an effective, low-energy Hamiltonian from the bond model. In the bond picture, for the system to transition from state $|1\rangle$ to $|2\rangle$ it can take different paths, for example $|1\rangle \to |3\rangle \to 2$, consisting of two hopping processes with an interim high-energy edge state. We will treat those processes perturbatively, as *virtual* excitations, and derive an effective hopping term between the two states $|1\rangle$ and $|2\rangle$. This effective hopping term is precisely the transverse field γ which flips the spin in the Ising picture, $-\gamma S_k^x = -\gamma \frac{1}{2}\left(S_k^+ + S_k^-\right)$.

A single QCA cell is described by the time-independent Schrödinger equation $H_k^c |\psi\rangle = E_k |\psi\rangle$, with $|\psi\rangle = [|\psi_P\rangle\, |\psi_Q\rangle]$. Our aim it to truncate the basis to $|\psi_P\rangle$ and derive and an effective Hamiltonian $\tilde{H}_k^c$ with the subspace Schrödinger equation $\tilde{H}_k^c |\psi_p\rangle = E_k |\psi_p\rangle$. The high-energy states $|\psi_Q\rangle$ have to be incorporated as virtual excitations. Using the basis depicted in Fig. 1.1 the single-cell bond Hamiltonian is very simple and can be written down explicitly. As the single-cell Hamiltonian is the same for all cells, we can drop the index k.

$$
H^c = \left(\begin{array}{cc|cccc}
V_0 & 0 & -t & -t & -t & -t \\
0 & V_0 & -t & -t & -t & -t \\
\hline
-t & -t & V_1 & 0 & 0 & 0 \\
-t & -t & 0 & V_1 & 0 & 0 \\
-t & -t & 0 & 0 & V_1 & 0 \\
-t & -t & 0 & 0 & 0 & V_1
\end{array}\right)
= \begin{pmatrix} H_{PP} & H_{PQ} \\ H_{QP} & H_{QQ} \end{pmatrix} \tag{1.4}
$$

Here, we have partitioned the Hamiltonian into four blocks, H_{PP}, H_{QQ}, H_{PQ}, and H_{QP}, corresponding to the low-energy subspace $|\psi_P\rangle$, the high-energy subspace $|\psi_Q\rangle$, and transitioning between the subspaces. With a this partitioned Hamiltonian the time-independent Schrödinger equation is

$$
\begin{pmatrix} H_{PP} & H_{PQ} \\ H_{QP} & H_{QQ} \end{pmatrix} \begin{pmatrix} \psi_P \\ \psi_Q \end{pmatrix} = E \begin{pmatrix} \psi_P \\ \psi_Q \end{pmatrix} \tag{1.5}
$$

Writing out the matrix equation as two equations explicitly and eliminating $|\psi_Q\rangle$ yields

$$
H_{PP} |\psi_P\rangle + H_{PQ} \frac{1}{E - H_{QQ}} H_{QP} |\psi_P\rangle = E |\psi_P\rangle \tag{1.6}
$$

and therefore

$$
\tilde{H}^c = H_{PP} + H_{PQ} \frac{1}{E - H_{QQ}} H_{QP} \,. \tag{1.7}
$$

Assuming that the system is predominantly in the subspace spanned by $|\psi_P\rangle$ and additionally that the hopping is very small, $t \ll V_0$, we can approximate $E \approx V_0$. We write out the matrix multiplications and use $H_{PP} = (V_0)_{ii}\,\delta_{ij}$, $H_{PQ} = (-t)_{ij}$, and so on. The effective Hamiltonian becomes

$$
\begin{aligned}
\tilde{H}^c_{ij} &= (V_0)_{ii}\,\delta_{ij} + (-t)_{ik}\,(V_0 - V_1)^{-1}_{kk}\,(-t)_{kj} \\
&= (V_0)_{ii}\,\delta_{ij} - \left(\frac{4t^2}{\Delta V}\right)_{ij} \,.
\end{aligned} \tag{1.8}
$$

As the system remains unchanged upon adding a constant term to the Hamiltonian, we can subtract the constant diagonal term $\tilde{H}_{ii} = V_0 - \frac{4t^2}{\Delta V}$, and arrive at

$$
\tilde{H}^c = \begin{pmatrix} 0 & -\frac{4t^2}{\Delta V} \\ -\frac{4t^2}{\Delta V} & 0 \end{pmatrix} \,. \tag{1.9}
$$

The off-diagonal matrix elements are the effective hopping, transitioning the system between its two states $|1\rangle \leftrightarrow |2\rangle$. If we now compare this matrix with the transverse field term of the Ising model, where we use the basis $|\downarrow\rangle \doteq |1\rangle$ and $|\uparrow\rangle \doteq |2\rangle$,

$$\begin{aligned} \tilde{H}^c &= -\gamma S_k^x \\ &= -\frac{1}{2}\gamma \left(S_k^+ + S_k^-\right) \\ &= \begin{pmatrix} 0 & -\frac{1}{2}\gamma \\ -\frac{1}{2}\gamma & 0 \end{pmatrix}, \end{aligned} \tag{1.10}$$

we identify the effective hopping as the transverse field γ

$$\gamma = \frac{8t^2}{\Delta V}\,. \tag{1.11}$$

The effective hopping γ is a virtual process, involving two hopping processes in the original bond model, yielding the t^2 in the numerator of the expression for γ, and an interim high-energy state gapped out by ΔV, hence the ΔV in the denominator. To arrive at the expression for the effective hopping we used the assumptions $\Delta V \gg T$ and $t \ll \Delta V$. As a reminder, $\Delta V = V_1 - V_0 = \frac{2-\sqrt{2}}{2}\frac{1}{a} \approx 0.3V_1$. Notably, the energy gap is independent of the compensation charge q. As the derivation used only a single cell, it is also implicitely assumed that the perturbations from other cells in the system are small, at least as far as the effective hopping is concerned. If the hopping depended on nearby cells' state, then the effective Hamiltonian would be much more involved and certainly could not be mapped to an Ising-like model.

We have successfully derived an effective hopping term and therefore also an effective two-state model for the QCA Hamiltonian. With only two states per cell the Hilbert space scales as $N_s = 2^{N_c}$ (N_c the number of cells) and up to 14 cells are computationally feasible, with memory requirements of 2GB. In practice we restrict the calculations to a maximum of 12 or 13 cells. For our calculations we can use the two-state approximation with the effective hopping term, but still retain the original cell-cell interaction term H_{kl}^{cc}. Summing up all cell-cell interactions exactly is no problem for the relatively small system sizes accessible with exact diagonalization. Thus, from a computational point of view, nothing is gained by expressing the cell-cell interaction as an Ising interaction. However, deriving J_{kl} from H_{kl}^{cc} is very rewarding conceptually and enables us to properly map the QCA approach to an Ising model. Additionally, an analytical expression for J_{kl} will already allow some key insights into the characteristics of QCA devices. Therefore, we now undertake the derivation of an expression for J_{kl}. The obvious starting point is the cell-cell interaction term H_{kl}^{cc},

$$
\begin{aligned}
H_{kl}^{cc} &= \sum_{\substack{i\in k\\ j\in l}} V_{ij}\,(n_i - q)\,(n_j - q) \\
H_{kl}^{cc} &= \sum_{\substack{i\in k\\ j\in l}} \frac{(n_i - q)\,(n_j - q)}{|\boldsymbol{R}_{kl} + \boldsymbol{r}_j - \boldsymbol{r}_i|} \\
&= \sum_{\substack{i\in k\\ j\in l}} \frac{n_i n_j - q(n_i + n_j)}{|\boldsymbol{R}_{kl} + \boldsymbol{r}_{ij}|}\,,
\end{aligned}
\tag{1.12}
$$

where i and j sum over the four dots $1\ldots4$ of cell k and l, respectively, $\boldsymbol{R}_{kl}$ denotes the vector between the centres of the cells, see Fig. 1.2(a). We have introduced $\boldsymbol{r}_{ij} = \boldsymbol{r}_j - \boldsymbol{r}_i$ and dropped the constant q^2 term. There are only four possible configurations for two interacting cells: $\uparrow\uparrow$, $\downarrow\downarrow$, $\uparrow\downarrow$, and $\downarrow\uparrow$. Using the shorthand notations $V_{ij} = \frac{1}{|\boldsymbol{R}_{kl}+r_{ij}|} + \frac{1}{|\boldsymbol{R}_{kl}-r_{ij}|}$ and $V_{00} = \frac{1}{|\boldsymbol{R}_{kl}|}$, we calculate their energies explicitely.

$$E^{\uparrow\uparrow} = (1-2q)\,(2V_{00} + V_{24}) - q\,(2V_{12} + 2V_{14}) \tag{1.13}$$

$$E^{\downarrow\downarrow} = (1-2q)\,(2V_{00} + V_{13}) - q\,(2V_{12} + 2V_{14}) \tag{1.14}$$

$$E^{\uparrow\downarrow} = (1-2q)\,(V_{12} + V_{14}) - q\,(4V_{00} + V_{13} + V_{24}) \tag{1.15}$$

$$E^{\downarrow\uparrow} = (1-2q)\,(V_{12} + V_{14}) - q\,(4V_{00} + V_{13} + V_{24}) \tag{1.16}$$

Note that the expression for two spin-down cells can be obtained from the expression for two spin-up cells (and similarly ($E^{\uparrow\downarrow}$ from $E^{\downarrow\uparrow}$) simply by rotating the system by 90°, or equivalently by permuting the dot numbering, $1,2,3,4 \to 4,1,2,3$. Symmetries can be exploited, for example $V_{43} = V_{12}$. Evidently, $E^{\uparrow\downarrow} = E^{\downarrow\uparrow}$, which, given the highly symmetric geometry of those cell arrangements, does not come as a surprise. But crucially, we find $E^{\uparrow\uparrow} \neq E^{\downarrow\downarrow}$. Therefore we have a system with three distinct energy levels which we cannot hope to represent with the solely two-level Ising term $J_{kl}S_l^z S_l^z$. Instead, let us try to map to a *modified* Ising model with a three-level cell-cell interaction term of the form

$$\tilde{H}_{kl}^{cc} = J_{kl} S_k^z S_l^z + J'_{kl}\,(S_k^z + S_l^z)\ . \tag{1.17}$$

For this Hamiltonian we have the energies

$$\tilde{E}^{\uparrow\uparrow} - \tilde{E}^{\uparrow\downarrow} = 2J_{kl} + 2J'_{kl} \tag{1.18}$$

$$\tilde{E}^{\downarrow\downarrow} - \tilde{E}^{\uparrow\downarrow} = 2J_{kl} - 2J'_{kl} \tag{1.19}$$

which yields

$$J_{kl} = \frac{1}{4}\left(\tilde{E}^{\uparrow\uparrow} + \tilde{E}^{\downarrow\downarrow} - 2\tilde{E}^{\uparrow\downarrow}\right) \tag{1.20}$$

$$J'_{kl} = \frac{1}{4}\left(\tilde{E}^{\uparrow\uparrow} - \tilde{E}^{\downarrow\downarrow}\right)\,, \tag{1.21}$$

and therefore, identifying $E^{\uparrow\uparrow} = \tilde{E}^{\uparrow\uparrow}, E^{\downarrow\downarrow} = \tilde{E}^{\downarrow\downarrow}$, and so on,

$$J_{kl} = \frac{1}{4}\left(4V_{00} + V_{13} + V_{24} - 2V_{12} - 2V_{14}\right) \tag{1.22}$$

$$J'_{kl} = \frac{1}{4}\left(1 - 2q\right)\left(V_{24} - V_{13}\right) . \tag{1.23}$$

These results, while abstract, are remarkable in two ways. First, the newly introduced term J'_{kl} vanished for $q = \frac{1}{2}$. In this case $E^{\uparrow\uparrow} = E^{\downarrow\downarrow}$. Thus, for charge neutral cells we recover the genuine, unmodified transverse field Ising model. Second, the Ising J_{kl} itself is independent of the compensation charge q. We will see that J_{kl} is the quadrupole-quadrupole cell interaction, to leading order. In a sense, it captures the pure QCA interaction. With the above equations we can also already look at rotational symmetries of J_{kl} and J'_{kl}: J_{kl} is invariant under rotations by 90° as can be seen by permuting the dots $1, 2, 3, 4 \to 4, 1, 2, 3$. This is what we expect intuitively. For example, a horizontal straight line of cells ($\theta = 0°$) should behave exactly the same as a vertical straight line of cells ($\theta = 90°$). In contrast, J'_{kl} is not invariant under rotations by 90°. In fact, applying the same dot permutation yields $J'_{kl} \xrightarrow{90°} -J'_{kl}$. Consequently, J'_{kl} is symmetric under rotations by 180°. It is also clear that a non-zero J'_{kl} breaks the system's symmetry under spin rotation, that is, $\tilde{H}^{cc}_{kl}$ from Eq. (1.17) is not unchanged under $\uparrow\uparrow \to \downarrow\downarrow$. This has profound implications for QCA. For non-zero J'_{kl} we would, for example, expect different polarization responses for two spin-down cells versus two spin-up cells. From an application point of view this is definitely not what we want. For QCA operation we therefore require charge neutral cells and a genuine, unmodified Ising model.

To obtain more tangible expressions for J_{kl} and J'_{kl} we do a multipole expansion of the V_{ij} terms. Specifically,

$$\begin{aligned} \frac{1}{|\boldsymbol{R}_{kl} \pm r_{ij}|} &= \frac{1}{R}\left(1 \pm 2\frac{\boldsymbol{r}_{ij}\hat{\boldsymbol{R}}}{R} + \frac{r_{ij}^2}{R^2}\right)^{-1/2} \\ &= \frac{1}{R}\left(1 \pm x + y\right)^{-1/2} \end{aligned} \tag{1.24}$$

is Taylor-expanded in x and y, keeping all terms up to $\mathcal{O}\left(\frac{a^4}{R^5}\right)$, which corresponds to quadrupole-quadrupole interactions. Plugging the results of the expansion back into Eq. (1.22) and (1.23) yields

$$J_{kl} = \frac{1}{32}\left(9 - 105\cos 4\theta\right)\frac{a^4}{R_{kl}^5} \tag{1.25}$$

$$J'_{kl} = \left(1 - 2q\right)\left(\frac{3}{2}\sin 2\theta\frac{a^2}{R_{kl}^3} + \frac{5}{4}\sin 2\theta\frac{a^4}{R_{kl}^5}\right) . \tag{1.26}$$

The leading order term of J_{kl} is R^{-5}, the quadrupole-quadrupole interaction. In contrast, the leading order term of J'_{kl} is R^{-3} and therefore, in general, J'_{kl} would be the dominating term—yet another argument why a non-zero J'_{kl} is highly undesirable for functioning QCA devices. Of course, we find our general symmetry observations confirmed by these more concrete expressions for J_{kl} and J'_{kl}: The former is invariant under 90° rotations, the latter only under rotations of 180°. Both terms vanish at select angles. For example, we have $J'_{kl} = 0$ for $\theta = 0°$, so that at least for an exactly straight line of cells we recover the unmodified Ising model, even for non-charge-neutral cells. This does not help when building more complex devices than a wire, of course, but might still be useful for some experiments. As another example, $J_{kl} = 0$ for $\theta = 22.5°$. Conceivably, this could be exploited for device applications, to decouple closely spaced cells. As multipole expansions the obtained expressions for J_{kl} and J'_{kl} should be valid for large cell-cell distances R. In principle, an arbitrary number of higher order terms can be included to make the expressions as exact as desired. In practice on the computer, however, we do not use the multipole expansion at all, but simply sum up all Coulomb interactions exactly. We will see in due course that for the small cell-cell distances we are typically interested in, an expansion up to R^{-5} is indeed not sufficient, and higher order terms would have to be included.

In summary, with the expressions for J_{kl} and J'_{kl}, (1.25) and (1.26), together with the earlier derived γ, Eq. (1.11), we have successfully mapped the QCA bond Hamiltonian (1.1) to a modified transverse field Ising model

$$\tilde{H} = -\sum_k \gamma S_k^x + \sum_{k<l} \left[J_{kl} S_k^z S_l^z + J'_{kl} \left(S_k^z + S_l^z \right) \right] . \tag{1.27}$$

1.4 Validity of the approximations

In the last three sections we have introduced three successive approximations for the QCA Hamiltonian, the fixed charge model, the bond model, and the Ising model. However, even though we know some theoretical limits in which those approximations become exact, we have given little thought to the practical limits, that is, parameter regimes where we can use the approximations and get sufficiently accurate results. Numerical benchmarks will help us establish these parameter regimes and also give us a better understanding of how the approximations behave in this parameter range.

The fixed charge approximation is a Hilbert space truncation where we only keep the states with exactly two electrons per cell. Fig. 1.3(a) compares the density of states of the fixed charge model against the exact grand canonical system. It reproduces the low-energy spectrum, in the plot up to $E \lesssim 35$, exactly. Therefore, as long as the two-electrons-per-cell sector is lowest in energy and the temperature is low compared to the energy gap to the next charge sector, the model works perfectly. Fig. 1.3(b) plots the number of particles per cell over temperature and demonstrates the breakdown of the approximation, precisely as the temperature does become comparable to this energy gap. Whereas the fixed charge model gives, per definition, a constant number of particles over the whole temperature

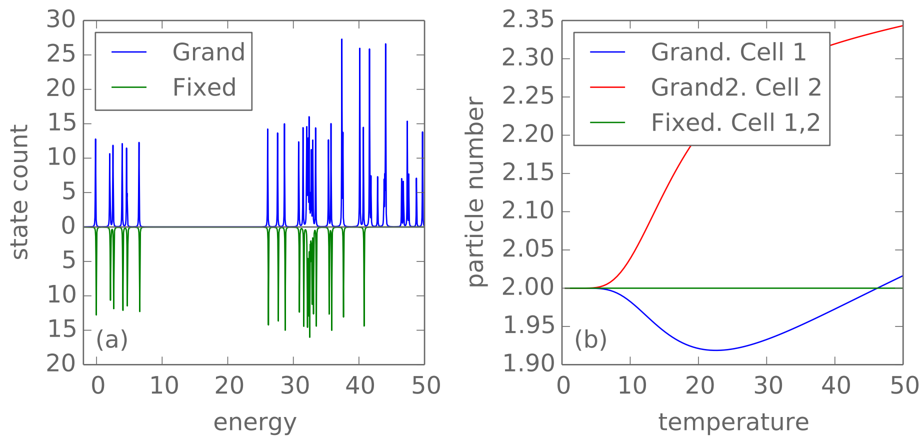

Figure 1.3: (a) Low-energy density of states of the exact grand canonical and the approximative fixed charge two-cell QCA system. For small energies the curves agree perfectly (up to $E \lesssim 35$). (b) Particle number per cell over temperature for the same two-cell system. The curves diverge for $T \gtrsim 10$.

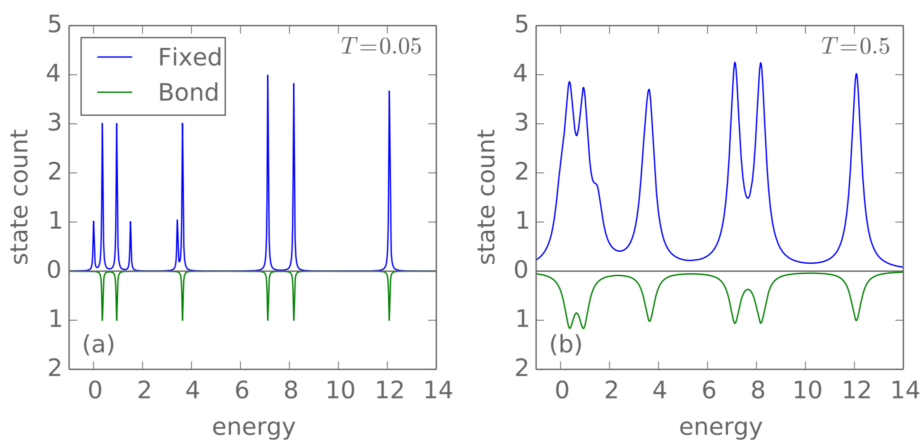

Figure 1.4: (a) Low-energy density of states of a one-cell QCA system for both the fixed charge and the bond model. The bond approximation only reproduces the triplet states, but omits the singlet states. The "measurement" temperature is indicated. (b) The same spectrum, but "measured" at a higher temperature. At large enough temperatures the singlet-triplet splitting is "washed out": The singlet and triplet peaks are no longer separately resolved and the bond model's state corresponds to four fixed charge states at roughly the same energy.

range, the grand canonical system's cell occupancy starts diverging from two electron per cell at around $T \sim 10$. This roughly corresponds to the energy states the fixed charge model missed at $E \sim 40$. A small deviation from exactly two electrons per cell is not detrimental to QCA, a cell occupied by only one or by three electrons, however, renders QCA non-functional. As we already said in the beginning of this chapter, we often use the fixed charge model as the starting point and assume, without further investigation, that a practical QCA implementation can be tuned to be in the right charge regime at a given temperature.

As a side note, we calculate the density of states graphs by folding the energy eigenvalues of the system—a delta function energy spectrum—with a Lorentzian with the half-width at half-maximum set by a "measurement" temperature. Very roughly speaking, this corresponds to a photoemission / inverse photoemission spectroscopy experiment at this temperature.

The bond model neglects doubly occupied states and represents the four states of a bond—one singlet and three triplets—with only one single bond state. The model thus assumes that singlet and triplet states are energetically degenerate, but we had already asserted that we might expect a small singlet-triplet splitting. Fig. 1.4(a) shows the density of states of a single QCA cell for both the fixed charge and the bond model. The nearest-neighbour Coulomb energy is $V_1 = 20$, the hopping is $t = 1$. A driver cell placed at a distance $d/a = 3$ to the left of the single cell sets an input. We have chosen the driver cell's polarization to be $P_D = 1$. Indeed, each bond state corresponds to three fixed charge states—the triplet—and one "close-by" state—the singlet. They are not energetically equivalent, but split by a small energy gap, ΔE_S, the singlet-triplet splitting. The bond model picks out the triplet states and in fact exactly reproduces those states. Just as the fixed charge model the bond model truncates the Hilbert space, but the retained states are exact. Evidently, the bond model keeps one of the three triplet states, but discards the other two triplet and the singlet states. We speculate that, similar to the antiferromagnetic Heisenberg coupling constant J emerging in the low energy limit of the Hubbard model (with $J \sim \frac{t^2}{U}$) [2], here, for the ground state virtual excitations to high energy doubly occupied states lower the energy of the singlet state compared to the triplet state. As the bond model misses those doubly occupied states it cannot accommodate singlet states and hence reproduces the triplet states. Consequently, we cannot hope that the bond model correctly reproduces ground state or low-energy properties. However, we assert that as long as the singlet-triplet splitting is "washed out", that is, as long as the temperature is much larger than the singlet-triplet gap, $T \gg \Delta E_S$, the approximation should give correct results. At high enough temperatures the system no longer "sees" the difference between the singlet and the triplet states. This is illustrated in Fig. **??**(b) where the spectrum is "measured" at a higher temperature. The singlet and triplets are no longer resolved separately. Instead, each bond state corresponds to four fixed charge states at roughly the same energy. The figure shows all six bond states of the single cell, the complete spectrum apart from the doubly occupied states. As this cell is perturbed by a nearby driver cell with $P_D = 1$, the ground state is qualitatively closest to the logic 1 state, or $|2\rangle$ in Fig. 1.1. Similarly, the first excited state is similar to $|1\rangle$, or logic 0, and the four higher energy states correspond to $|4\rangle$, $|5\rangle$, $|3\rangle$, and $|6\rangle$, in that order. Of course, in general the energy eigenstates are a mixture of all basis states, but we can still characterize them by their most dominantly contributing basis state. As this a non-charge-neutral system $q = 0$ with a relatively small cell-cell distance $d/a = 3$, charge buildup tends to push the electrons to the far edge of the cell, thus making $|4\rangle$ lower in energy than $|6\rangle$.

Since the bond model ignores the singlet-triplet splitting it is important to understand how the gap ΔE_S depends on various system parameters. To that end we picked out a few selected singlet-triplet states from the spectrum in Fig. 1.4(a) as examples. Contrary to expectations, for those states the gap ΔE_S did not change significantly with the on-site Coulomb repulsion U, however, it did decrease with decreasing d, the cell-cell distance. Most importantly, for the nearest-neighbour Coulomb energy V_1 we found $\Delta E \sim \frac{1}{V_1^p}$. The exponent is $p \sim 3$ when the cell "sees" a biasing external potential (e.g. $P_D = \pm 1$) and $p \sim 1$ otherwise (e.g. $P_D = 0$). Even though our method is anything but rigorous and the obtained results very likely not universally true, the findings should nonetheless give a good enough idea of the principle trends. Quite generally, the higher the overall Coulomb potential (large V_1, small d), the smaller the singlet-triplet splitting and, conceivably, the more accurate the bond approximation. Consequently, we expect the approximation to work as long as the singlet-triplet splitting is "washed out," that is, as long as the temperature is much bigger than the gap ΔE. As a very, very rough estimate we come up with $T \gg \frac{t^2}{V_1}$. Of course, we also need $T \ll U$ so that the doubly occupied states are gapped out. Outside of this loosely defined regime, the bond model can and does go terribly wrong.

To illustrate the limitations of the bond approximations we now look at a two cell system: a straight horizontal line of two cells with a driver cell to the left. Fig. 1.5 shows the spectra and output polarizations of a two-cell wire for two different Coulomb energies, $V_1 = 20$ and $V_1 = 100$. Otherwise the parameters are the same as for the one-cell system in the previous graph. In particular, the spectrum in Fig. 1.5(a) is exactly the same as in Fig.1.4(a) except that we have added one more cell to the system. Each bond state now corresponds to 16 $(4 \cdot 4)$ fixed charge states. Looking at the four lowest-energy peaks in the spectrum, we see that the bond model exactly reproduces the 9 triplet-triplet states, but misses the three singlet-triplet and the three triplet-singlet states (in the graph the corresponding two peaks are hardly distinguishable), as well as the single singlet-singlet ground state. The four lowest bond states should roughly correspond to both cells being aligned with the driver cell (the ground state), only one of the two cells being aligned with the driver cell, and both cells being anti-aligned with the driver cell. Higher energy states have at least one of the cells not in the preferred diagonal states $|1\rangle$ and $|2\rangle$, with electrons occupying predominantly the edge of a cell. Arguably, the spectra of the fixed charge and the bond model in Fig. 1.5(a) do not look very similar. Consequently, the polarization curves in Fig. 1.5(b) do not agree, especially at low temperatures. In fact, it is rather remarkable that given the widely dissimilar spectra the polarizations actually do agree relatively well at higher temperatures, $T > 1$. The bond model only reproduces the most populous energy states of the exact spectrum. Apparently, that is enough to give (almost) correct results at high temperatures. The lower the temperature, the more important become the few lowest lying energy states which the bond model misses. Very roughly speaking, the temperature where the bond model's polarization becomes accurate also matches the temperature where we saw the singlet-triplet splitting being washed out in Fig. 1.4(b), they are at least of the same order of magnitude. For the much larger Coulomb energy $V_1 = 100$ the spectra look much more alike, qualitatively, even though the bond model obviously still does not resolve all the lines of the exact density of states, and consequently the approximation works much better, Fig. **??**(a) and (b). The polarization curves agree down to much lower temperatures and even the discrepancy for the ground state polarizations is much reduced. Compared to the $V_1 = 20$ system the ground state polarization is much larger and, generally, the higher the cell polarization, the better the agreement between bond and fixed charge model. We also note that in the spectrum the peaks are much more spaced out, compared to the $V_1 = 20$ system. Thus the system retains larger cell polarizations up to much higher temperatures.

The polarization of the fixed charge model shows a curious bump at low temperatures, for example in Fig. 1.5(b) and similarly, if less visibly, in Fig. 1.5(d). Apparently, the ground state is not the most polarized state. Maximum polarization is reached at a small, but finite temperature. At the same time, for the bond model the ground state is the most polarized state and generally its $T = 0$ polarization is larger than that of the fixed charge model. Interestingly, the bond model's ground state polarization is largely independent of the magnitude of the driver polarization and also only weakly influenced by the cell-cell distance d, especially for charge-neutral cells where no charge buildup occurs. Instead, it is predominantly set by V_1, and thus by V_1/t and the energy gap $\Delta V = V_1 - V_0$. Without an external perturbation such as a non-zero driver polarization the ground state polarization is zero, of course. But any infinitesimal external perturbation will instantly see the bond model's ground state polarization snap to its full value. We interpret this behaviour as the ground state actually consisting of two energetically degenerate states, corresponding to $\pm P_{gs}$, where P_{gs} is the full ground state polarization for a given V_1. The smallest perturbation lifts this degeneracy and sees the system snapping to either $+P_{gs}$ or $-P_{gs}$. Now the bond model's ground state corresponds to the fixed charge model's triplet state—one of the lower lying excited states, but not the ground state. The true ground state of the more exact model is a single singlet state, a superposition of the $+P_{gs}$ and $-P_{gs}$ (and other) states. Therefore the polarization of the true ground state is generally smaller in magnitude than the polarization of the corresponding two triplet states, explaining the low temperature bump in the polarization curve and the larger polarization of the bond model's ground state.

The Ising approximation is derived as an effective low-energy model from the bond

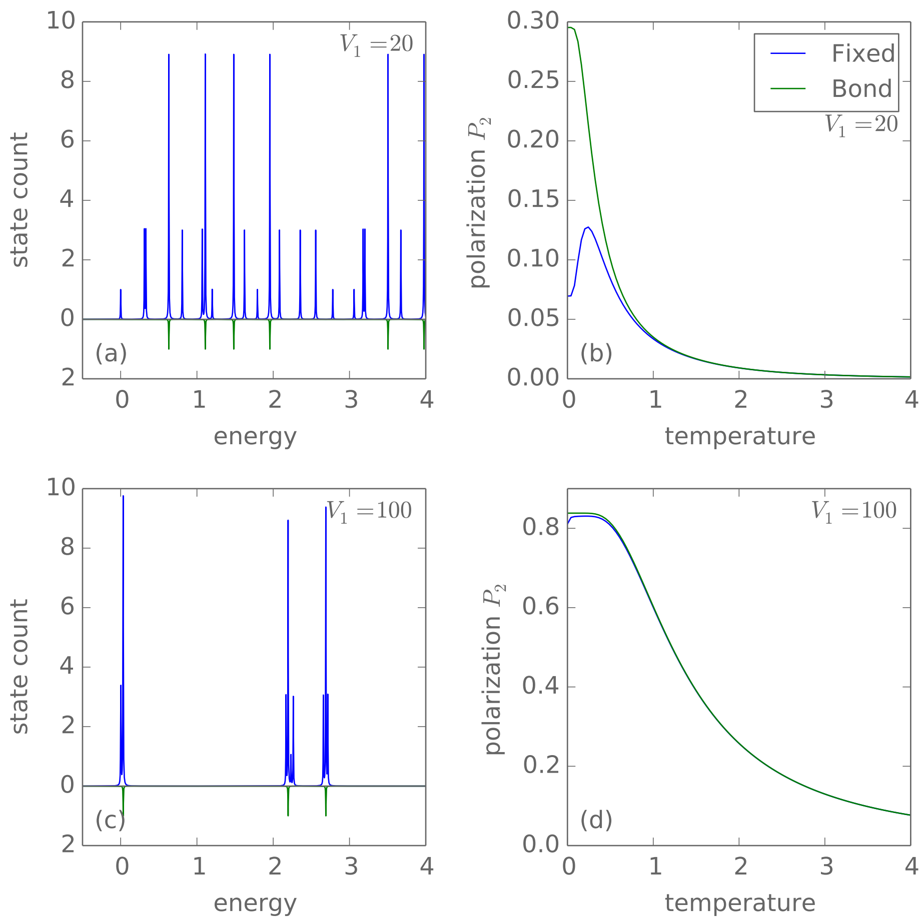

Figure 1.5: The two-cell fixed charge and bond systems at $V_1 = 20$ and $V_1 = 100$. (a)(c) Low-energy density of states. (b)(d) Output polarization P_2 over temperature. For a small Coulomb repulsion the density of states curves look qualitatively very different (a) and the bond approximation does not work very well (b). At a larger Coulomb repulsion the density of states curves look much more alike (c) and the bond approximation works much better (d).

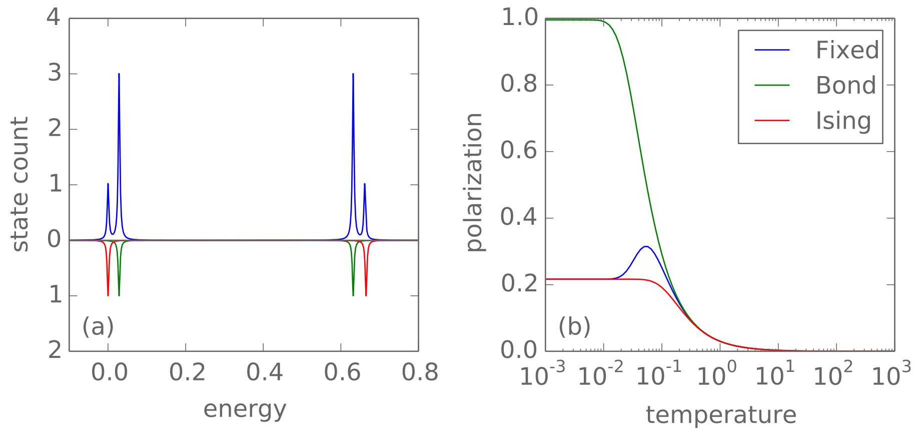

Figure 1.6: ...

Hamiltonian. It is therefore qualitatively different from the previous two approximations: It is not merely a Hilbert space truncation. *A priori* its states need not exactly correspond, neither energetically nor qualitatively, to either the bond or the fixed charge model. Of course, in the limit where the assumptions in the derivation become exact, the Ising model's states should resemble the bond model's states accurately. Specifically, the derivation assumed $E \approx V_0$ (E the energy of the whole system) and therefore $t \ll \Delta V$, as well as $\Delta V \gg T$. The neglected edge states need to be gapped out. Additionally, cells are assumed to be isolated, so the Ising model presumably requires reasonably large cell-cell distances. The Ising model also inherits the limits of the bond model and we would expect $T \gg \Delta E_S$ and $T \ll U$ as requirements for the Ising model as well. It is important to keep in mind that the Ising model is not a low-energy model for the more exact fixed charge Hamiltonian—it is derived as the low-energy limit of the bond model, which, however, is not an accurate low-energy description of the fixed charge system. The Ising model with its only two states per cell can never accurately capture the lowest lying states of the fixed charge model, which are, for a multi-cell system, a mixture of singlet-triplet states across cells. The approximation can also not hope to capture non-charge neutral systems and more specifically charge buildup correctly. It simply lacks the edge states that would be the manifestation of charge buildup, as discussed in the example of the one-cell bond system above. We had seen in the derivation of the Ising model that the lack of charge-neutrality is very problematic for the QCA approach in general. Consequently, we will concentrate on charge neutral systems, $q = \frac{1}{2}$, for the remainder of the chapter. For the following calculations we do not use the derived J_{kl} and J'_{kl} terms, but some all Coulomb interactions exactly.

To understand how the Ising approximation works we again start by looking at the

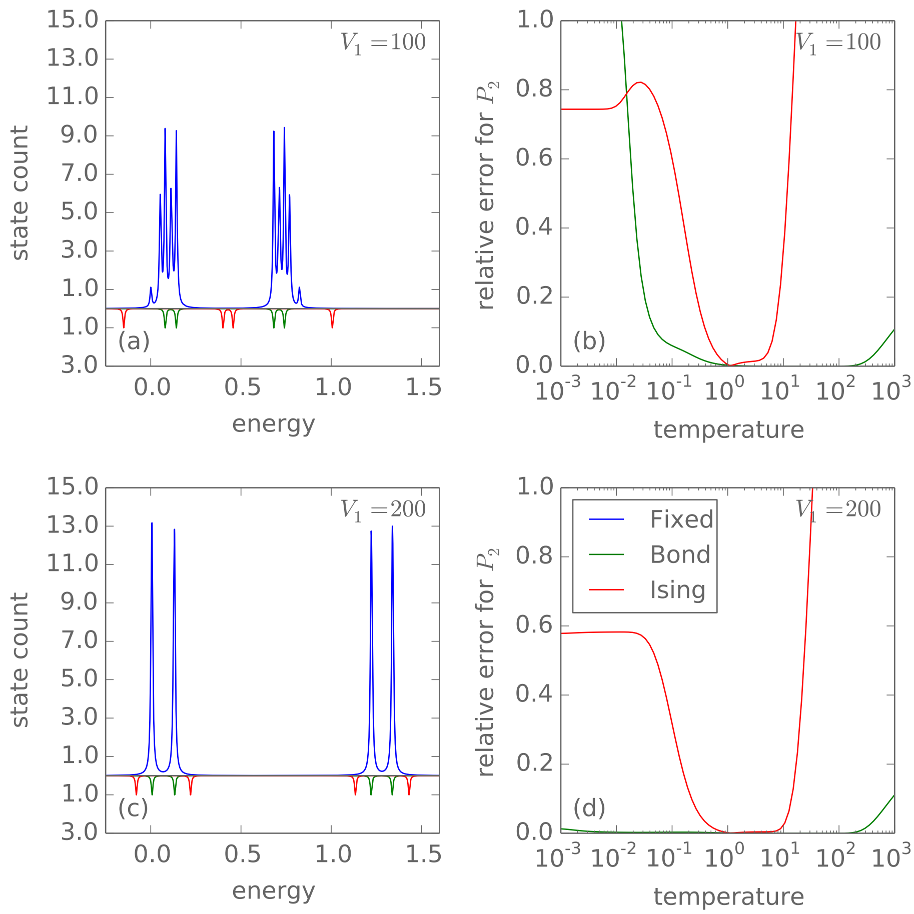

$V_1 = 100$
$V_1 = 200$
state count
energy
relative error for P_2
temperature
(a)
(b)
(c)
(d)
Fixed
Bond
Ising

Figure 1.7: ...

density of states for a one-cell system, Fig. 1.6(a). We have plotted both the fixed charge and the bond model for comparison and now use slightly different system parameters. The nearest-neighbour Coulomb energy is $V_1 = 100$, the cell-cell distance is $d/a = 4$, the driver cell is only slightly polarized with $P_D = 0.1$, and, as always, the hopping is $t = 1$. We are in for a surprise! Evidently, the Ising model reproduces the singlet states and not the bond model's triplet states. In line with this observation, the Ising model exactly matches the fixed charge model's ground state polarization, but misses the triplet-bump at $T \sim 0.05$, Fig. 1.6(b). Thus, for the one-cell system the Ising approximation unexpectedly captures the system's ground state correctly. Apparently, even though we had derived the Ising model from the bond Hamiltonian, it does not really resemble the bond model. Instead its states are of singlet character. It even gets the ground state right, after we had just asserted that it cannot possibly be a low-energy description of the fixed charge model. In short, the Ising model's behaviour is very confusing. To lift the confusion, we first note, that even though the Ising model correctly captures the ground state of the single cell system, this is not true in general, for larger systems, as we will see in a moment. It also is not a low-energy effective model, because even for the one-cell system it only reproduces the ground state, but not the first and second excited states. Second, we need to be very careful when we talk about the bond model. The bond Hamiltonian is simply a spinless model that does not distinguish between singlet and triplet states. In contrast, the bond model uses a concrete basis and we saw that it chooses the triplet states. Therefore, the bond Hamiltonian, from which we derived the Ising model, and the bond model are not equivalent. With its choice of basis the Ising model captures the singlet states. This makes sense in so far as the Ising model is derived as the low-energy effective model and the singlet states are the lowest energy states. The Ising and bond model states are therefore different energetically and qualitatively. Still, in the limit where the Ising model becomes exact, the singlet-triplet splitting should go to zero and the states of the two models will become equivalent. On second thought, the fact that the Ising model exactly reproduces the ground state of the one-cell system is maybe not as surprising: We had derived the Ising model precisely for a single cell and as it captures the singlet states, that is what we get. Apparently, the perturbation of the external driver cell does not change that fact. Close inspection of the energy gap between the Ising model's only two states, however, as compared to the equivalent energy gap between the fixed charge model's two lowest energy singlet states, show that the fixed charge and Ising states are not exactly the same, energetically. The difference is hardly discernible in the plotted spectrum, but more pronounced for different system parameters. This is not surprising, given that the Ising approximation is a effective model and used several assumptions in its derivation. Indeed, for the single-cell system we can study the energy gap for the Ising as compared to the fixed charge model and find that they are in better agreement for larger V_1, smaller t, and larger cell-cell distance d/a (although the difference becomes constant for large enough d/a, presumably when the cells are spaced far enough apart to not influence each other's hopping), exactly confirming the assumptions and limits of our derivation.

To be able to better quantitatively compare different models over a wide range of temperatures and independent of the magnitude of the polarization, we introduce the relative error of the polarization, defined as, for the Ising model,

$$\epsilon_k^I = \frac{\left|P_k^F - P_k^I\right|}{P_k^F} \, . \tag{1.28}$$

Here, P_k^F refers to the polarization for cell k with the fixed charge model and P_k^I is the same polarization, but determined using the Ising model. The relative error for the bond model, ϵ_k^B, is defined equivalently. For meaningful comparisons between the different models' polarizations it is important not to fully polarize the cells. Once we push the system into a regime where we have $|P_k| \sim 1$, the cells are saturated and the models tend to agree. This is why we have, for our calculations with the Ising model here, which generally requires larger V_1/t ratios, chosen a larger cell-cell distance and a smaller driver cell polarization.

Fig. 1.7 shows the relative error together with the density of states for all three models for a two-cell system at $V_1 = 100$ and $V_1 = 200$. As before we find that the bond approximation works much better when its spectrum looks qualitatively more similar to the fixed charge spectrum. At $V_1 = 100$ the bond model yields a almost fully polarized ground state, whereas the fixed charge model's $T = 0$ polarization is much smaller, resulting in a very large relative error as indicated in Fig. 1.7(b). At $V_1 = 200$, Fig. 1.7(d) both fixed charge and bond are almost fully polarized at low temperatures and the relative error is therefore very small. For these calculations we have used $U = 1000$ (before we used $U = 10^6$) and indeed we can see that the bond model starts to diverge for $T \gtrsim 200$. Even at $T = 1000$ the error is relatively small, because the polarization is quite insensitive to doubly occupied dots, being defined solely as the difference in charge of one diagonal versus the other diagonal of the cell. Note that at these large temperatures the actual polarization is already very, very small. Looking at the relative error of the Ising model we first notice that it becomes very, very large for $T \gtrsim 5 \ldots 10$. Of course, this is a consequence of the Ising model missing the gapped out edge states, where the gap is $\Delta V \sim 0.3 V_1$. Accordingly, the upper temperature limit for a small relative error is larger for $V_1 = 200$ than for $V_1 = 100$, though maybe not by as much as we might expect. In contrast to the one-cell system, for two cells the ground state of the Ising model no longer agrees with the ground state of the fixed charge model. The Ising model's $T = 0$ polarization is generally smaller than the polarization of the exact model. Similarly to the bond model the relative error of the ground state polarization decreases for larger V_1. We asserted before that we never expected the Ising model to get the low-temperature behaviour right and in this light, the surprising agreement of the ground state for the one-cell system can be viewed as a curious coincidence, related to the details of how exactly we had derived the Ising model. Most importantly, the relative error curves of the Ising model reveal that the temperature range where the error is actually small—that is, where the Ising model can be considered valid—is quite narrow. For $V_1 = 100$ it is almost like a sweet spot, a very narrow window around $T \sim 1$, where the error is close to zero. For $V_1 = 200$ the situation is much better, the error is small in the temperature range $T = 0.8 \ldots 8$. Generally, the temperature range where the error is small only very weakly depends on the cell-cell distance d/a or the driver polarization P_D. It is mostly set by V_1 (and as before we always keep the hopping fixed to $t = 1$). Roughly speaking, the lower temperature limit is set by the singlet-triplet splitting, which becomes smaller with increasing V_1, and the upper temperature limit is set by ΔV which is, of course, directly proportional to V_1. If we analyse the relative error at a fixed temperature, in the temperature regime where the error is small and the model can be considered valid, we find, similarly to the our observations for the one-cell system, that the error decreases with increasing V_1. However, there is no clear trend for the error when changing the cell-cell distance d/a, except that the d/a cannot be very, very small, $d/a < 2$, because then the Ising approximation breaks down. The spectra of the Ising model do not compare well the fixed charge or even the bond model. Especially at $V_1 = 100$, the Ising model's density of state curve looks widely dissimilar to any of the two other models. Clearly, the Ising approximation gets the energy levels completely wrong. However, when evaluating the spectrum we should keep in mind that, in contrast to the bond model, the Ising model's state need not be the same qualitatively as the more exact models' states. This explains that even though the spectrum looks completely wrong the Ising model does work, if in a very small temperature range. Still, in the right limit the Ising model should eventually resemble the bond model. Accordingly, at $V_1 = 200$ the spectra do look more agreeable, even though the Ising model still is far from an accurate reproduction of the bond spectrum. The qualitative agreement of the spectra becomes better for smaller cell-cell distances and larger driver cell polarizations as well, thus generally when the cells are more fully polarized.

All told, the Ising model is a tricky approximation. It is conceptually confusing, because, even though it is derived from the bond Hamiltonian, it does not exactly resemble the bond model. Adding to this confusion is the fact that it gets the ground state of the one-cell system right, but, as expected, not for larger systems. From a practical point of view, the Ising model requires very large V_1/t ratios and its operational window can be very, very small. Great care should thus be exercised when using the Ising approximation for calculations. Ising model calculations should be verified with a more exact model as much as possible and the error, and trends of the error, should be kept in check. Where an explicit verification is not possible, for larger systems, its result should be taken with a grain of salt.

As a final step, we look at a few concrete systems—three-cell to five-cell wires—and trends of the error of the Ising model for these systems. For a horizontal line of cells with three to five cells with a cell-cell distance of $d/a = 4$ and a nearest-neighbour Coulomb energy $V_1 = 100$, Fig. 1.8(a) shows the relative error as a function of the number of cells, that is, the wire length at two different temperatures. For these larger systems the Ising model and hence its error is benchmarked against the bond model, and not the fixed charge model as before. We notice that for these larger systems the error is quite a bit smaller for

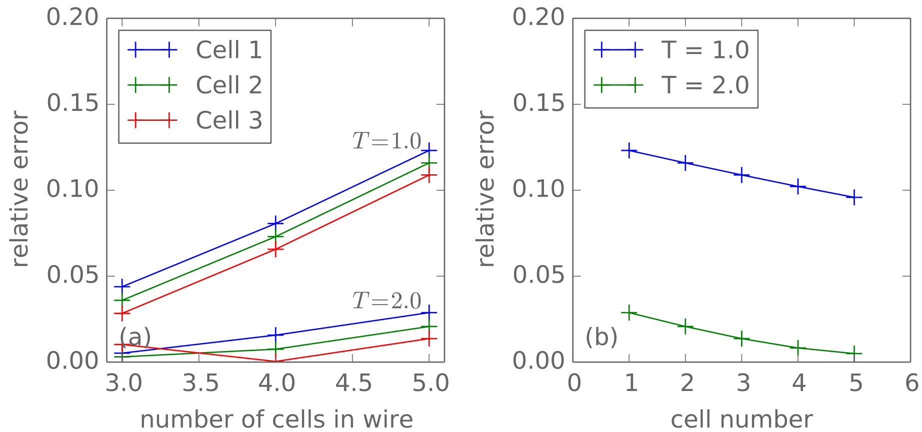

Figure 1.8: ...

the slighter higher temperature, at $T = 2$. In fact, for an error smaller than 10% we have to choose $T = 2$. Most worryingly, the error grows with the number of cells in the wire. This trend holds quite generally, for a range of systems with different cell-cell distances d/a and Coulomb energies V_1. For larger systems we expect the error to become large as well and unfortunately there is nothing we can do about it. For large systems we will not be able to compare the Ising model to the bond model and we will not be able to give a good upper bound for the error. The error will therefore become uncontrolled. On a slightly more optimistic note, we notice that the error seems to decrease from cell to cell inside each wire. This is explored in more detail in Fig. 1.8(b), where we have plotted the error of each cell polarization inside a five-cell wire. Evidently, the error decreases along the wire and we can expect this decrease to counter the generally growing error for longer and longer wires, at least as long as we are interested only in the output polarization of the wire. For wires with smaller cell-cell distances the error does not always decrease along the wire, but at least it does not seem to increase either. For this particular QCA structure for the chosen system parameters we are relatively confident that the error of the output polarization, while not well controlled, will at least not grow very large for systems accessible with the Ising approximation—up two twelve QCA cells.

In this chapter we introduced and established three approximations for QCA systems, the fixed charge, the bond, and the Ising model. We usually use the fixed charge model as the starting point, without further explicit verification. In principle, whether the fixed charge approximation holds for some chosen set of parameters has to be checked for each potential QCA implementation on a case by case basis. If the fixed charge model is not applicable, then there is also generally no hope of implementing QCA on the given experimental system. At high temperatures the bond approximation is a very good description of QCA systems. It starts breaking down when the temperature becomes comparable to the singlet-triplet splitting and therefore for small V_1 and too large cell-cell distances. We generally assume doubly occupied states to be sufficiently gapped out (U is practically infinite) and can safely neglect them, as the bond model does. While it is conceptually deeply rewarding to map QCA to an Ising system, we have seen the Ising approximation to be difficult to handle and control for practical calculations. It is only valid in a relatively small parameter window and great care has to be taken with its application. Generally speaking, both the bond and the Ising approximation become exact in the same limits—large V_1/t, small (but not too small) cell-cell distances—and not coincidentally those are the limits where the QCA approach works best, too. Both approximations are useless for low-temperature calculations, and for ground state properties we thus have to turn to the fixed charge model, which, however, only allows system sizes of up to three or four cells. We will use the bond model for most of our QCA characterization work at finite temperature. With system sizes of up to six cells it already allows some interesting insights. The Ising model is problematic and we will employ it sparingly, to look at larger structures such as gates.

Bibliography

[1] A. W. Sandvik, "Stochastic series expansion method for quantum Ising models with arbitrary interactions," *Phys. Rev. E* **68** (Nov, 2003) 056701. `http://link.aps.org/doi/10.1103/PhysRevE.68.056701`.

[2] A. Auerbach, *Interacting electrons and quantum magnetism*. Graduate texts in contemporary physics. Springer New York, 1994. `http://books.google.ca/books?id=tiQlKzJa6GEC`.